

Numerical Simulation of Oxidation Effects in Laser Cutting of Mild Steels

Kai Chen, Y. Lawrence Yao
Dept. of Mechanical Engineering
Columbia University
New York, NY 10027

Abstract

A numerical model is developed to simulate the process of oxygen-assisted laser cutting of mild steels. The coupled concentration and energy balance equations are solved by a control-volume based computational scheme while the velocity field is obtained by the analytical boundary theory. The enthalpy method is adopted to trace the free boundary of phase change. The steady-state simulation results reveal such details as the temperature profile at the cut front, the effects of impurity gas on the cutting speed, reaction energy, and heat affected zone. The striation phenomenon is simulated through the oscillation of the oxide layer caused by hydrodynamic instability. The temperature fluctuation range versus cutting speed and pressure shows similar trends as the experimental results of striation depth.

Nomenclature

c : molar density	c_p : heat capacity
D : diffusion coefficient	$D_{0,m}$: diffusion constant
E_a : reaction energy	ΔG_{rx} : standart Gibbs free energy
H : kerf width	ΔH : latent heat content
ΔH_r : reaction energy	h : thickness of molten layer
h_m : latent heat	K : thermal conductivity
K_c : equilibrium constant	k_r : kinetic rate coefficient
k_o : kinetic rate constant	M : molecular weight
N : mass flux	P : gas pressure
q_r : reaction heat flux	R : universal gas constant
T : temperature	T_m : melting temperature
t : time	U : bulk gas velocity
u : cutting speed	V : diffusion volume
V_s : surface velocity	v : velocity in y direction
v^* : friction velocity	X : oxygen concentration
x : distance perpendicular to melt flow	y : distance along melt flow
ρ : density	δ : thickness of gas diffusion film
μ : viscosity of melt	ν : kinematic viscosity

Subscripts:

e: equilibrium state

i: reaction plane

n2: nitrogen

s: melt surface

g: gas phase

m: melt phase

o2: oxygen

δ : interface of bulk gas and gas diffusion film

1. Introduction

Laser cutting, as one of the most common manufacturing processes involving laser, has made headway into well established areas of manufacturing. Meanwhile, the modeling of laser cutting has been addressed by a number of investigators to help understand the basic mechanism involved and to predict the important parameters and phenomena. However, most of the modeling work pertain only to inert gas cutting, while in majority of industrial practice, laser cutting of mild steel uses oxygen as an assist gas to provide exothermic energy and to help remove the molten metal. When dealing with oxygen assisted cutting, the existing models either assume a lumped percentage of material participating in the reaction, or use oversimplified assumptions with certain parameters difficult to determine (Shuocker and Abel, 1984; Di Pietro and Yao, 1995). This has limited accurate predictions and better understanding of cutting mechanisms associated with oxidation. One important phenomenon in oxygen-assisted cutting is the formation of striations, which has received much attention since the early stage of laser cutting because it strongly affects the cut quality (Arata, *et al.*, 1979). The explanations given for this phenomenon have been hydrodynamic instability (Vicanek, *et al.*, 1986), internal instability of the cutting process (Shuocker, 1986), cyclic oxidation (Ivarson, *et al.*, 1994), and more recently cyclic oxidation caused by hydrodynamic instability (Chen and Yao, 1997). It will be of interest to numerically simulate the striation phenomenon.

This paper presents an oxidation model based on heat transfer, transport and chemical rate theory. By solving the coupled energy and concentration equations, the model is capable of describing the details of oxidation process and estimating important effects such as reaction energy, the purity of oxygen on cutting speed. The energy balance equation is written in the form of enthalpy to deal with the phase change. The velocity field is obtained by balancing the shear stress at the interface. The steady-state model is further expanded to a dynamic one. By oscillating the oxide layer according to the instability theory of hydrodynamics (Chen and Yao, 1997), one is able to observe the oscillation of the oxidation process which causes the temperature fluctuation during the cutting process.

2. Theoretical Background

2.1 Physical Model

A simplified model is shown in Figure 1. The workpiece is fed at a constant speed in a direction perpendicular to the focused laser beam. Laser irradiation together with the reaction energy heats up the metal and the gas jet exerts momentum on the molten

material, leading to the ejection of the melt. The calculation domain is shown in the picture. The solid and liquid are assumed to be isotropic with homogeneous properties.

The chemical reaction is assumed to be of heterogeneous type and takes place at a single plane. The mass transfer in the oxidation process mainly consists of a. the mass transfer from the bulk gas phase to the melt surface; b. the mass transfer in the reacted layer; c. the first order reaction at the reaction plane (Figure 1). In our study, the simulation consists of two stages: the steady-state calculation that takes off the oxide layer and assumes that the reaction occurs at the gas-liquid interface, and the time-dependent calculation that assumes the growth of the oxide layer follows the well known parabolic law for diffusion controlled reaction, and the oxide layer is removed by hydrodynamic forces. The input heat sources are the absorbed laser heat and the exothermic reaction heat. Heat is lost from the cutting zone by conduction, phase change and convection. The radiative heat loss is neglected.

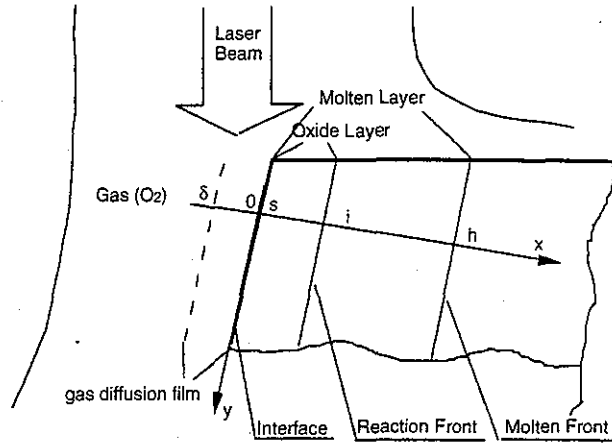


Figure 1: Physical model and calculation domain

2.2 Governing Equations and Boundary Conditions

a. Mass Balance

The governing equation for mass transfer in the gas phase is (diffusion in y direction and convection in x direction are neglected):

$$c \frac{\partial X_{o_2}}{\partial t} + cv \frac{\partial X_{o_2}}{\partial y} = - \frac{\partial}{\partial x} N_{o_2} \quad (1)$$

The oxygen diffusion consists of the molecular diffusion and the net bulk convection (Fick's Law). Assuming a small amount of impurity gas (e.g. nitrogen) existing, the molar flux of oxygen is expressed as:

$$N_{o_2} = -cD_{o_2,g} \frac{\partial X_{o_2}}{\partial x} + X_{o_2}(N_{o_2} + N_{n_2}) \quad (2)$$

It is reasonable to assume that no impurity gas enters into the oxide layer, thus $N_{n_2} = 0$, and Eq. (1) can be rearranged to yield:

$$\frac{\partial}{\partial x} \left(- \frac{cD_{o_2,g}}{1 - X_{o_2}} \frac{\partial X_{o_2}}{\partial x} \right) = cv \frac{\partial X_{o_2}}{\partial y} \quad (3)$$

In our transient calculation, a thin oxide layer with large resistance exists and the oxygen must diffuse through the liquid oxide layer before chemical reaction takes place. The reaction is thus diffusion controlled and is largely dependent on the behavior of the oxide layer. The governing equation for mass transfer in liquid oxide phase is:

$$c \frac{\partial X_{o_2}}{\partial t} + cv \frac{\partial X_{o_2}}{\partial y} = \frac{\partial}{\partial x} \left(cD_{o_2,m} \frac{\partial X_{o_2}}{\partial x} \right) \quad (4)$$

The boundary condition for the above described mass transfer is a) $X_{O_2} = X_{O_2, \text{bulk}}$ at the bulk gas stream; b) The chemical reaction at the interface, which is of the first order and follows

$$N_{O_2} = k_r c (X_{O_2, i} - X_{O_2, e}), \quad (5)$$

where the kinetic rate constant has an Arrhenius temperature dependence:

$$k_r = k_{r0} \exp(-E_a / RT). \quad (6)$$

The equilibrium concentration $X_{O_2, e}$ is obtained from the equilibrium constant K_e which is determined by Gibbs free energy of the reaction:



$$\Delta G_{rx}^{\circ} = -RT \ln K_e. \quad (8)$$

b. Energy Balance

The governing equation for heat transfer in the gas phase is in the parabolic form which is similar to the case of mass transfer:

$$\rho_g \frac{\partial c_p T}{\partial t} + \rho_g v \frac{\partial c_p T}{\partial y} = \frac{\partial}{\partial x} (K_g \frac{\partial T}{\partial x}) \quad (9)$$

The equation for heat transfer involving phase change in the material can be expressed in the enthalpy formulation:

$$\frac{\partial \rho h}{\partial t} + \frac{\partial \rho \Delta H}{\partial t} + \frac{\partial \rho v h}{\partial y} + \frac{\partial \rho u \Delta H}{\partial x} = \frac{\partial}{\partial x} (K \frac{\partial T}{\partial x}), \quad (10)$$

h is the sensible enthalpy defined as $h = h_{ref} + \int_{T_{ref}}^T c_p dT$. ΔH is the latent heat content. It may vary as h_m (latent heat) or zero, depending upon whether the temperature exceeds the melting temperature. For simplification, it is assumed that the melting temperature is the melting point of pure iron (1527 °C). The reaction heat source is obtained from:

$$q_r = 2\Delta H N_{O_2}. \quad (11)$$

The boundary conditions for energy balance are that both the bulk gas temperature and the solid temperature far away from heat sources are equal to ambient temperature.

c. Momentum Balance

Instead of solving complex two phase Navier-Stokes equations, the velocity field is obtained from the results of analytical boundary theory. For the gas phase, the air velocity profile close to the liquid surface is assumed to be the same as that for turbulent flow in a smooth-walled channel. The $1/7^{\text{th}}$ -power velocity-distribution law is adopted here (Schlichting, 1979).

$$\frac{v}{v^*} = 8.74 \left(\frac{xv^*}{v_g} \right)^{\frac{1}{7}}, \quad (12)$$

where v^* is the friction velocity determined by

$$\frac{U}{v^*} = 8.74 \left(\frac{Hv^*}{2v_g} \right)^{\frac{1}{7}}. \quad (13)$$

The velocity profile in the melt phase is assumed to be linear and the surface velocity V_s is determined by

$$\rho_g v^{*2} = \frac{\mu V_s}{h}. \quad (14)$$

2.3 Physical Properties

Most of physical properties are temperature dependent and need to be updated during the calculation. The diffusivity of oxygen in the gas phase $D_{O_2,g}$ is not affected by concentration for low to moderate pressure (<10 atm). It is dependent on the absolute temperature, the molecular weight and the diffusion volume of the impurity gas, and can be correlated as (Nickolas, 1995):

$$D_{O_2,g} = \frac{0.001T^{1.75} \left(\frac{1}{M_{O_2}} + \frac{1}{M_{n_2}} \right)^{1/2}}{P(V_{O_2}^{1/3} + V_{n_2}^{1/3})^2} \quad (15)$$

The diffusivity of oxygen in the liquid phase takes the form of

$$D_{O_2,m} = D_{O,m} \exp(-E_a / RT) \quad (16)$$

The diffusivity of oxygen in liquid FeO is about $4 \times 10^{-4} \text{ cm}^2/\text{s}^{-1}$ at 1550°C . It may however reduce as the ferric iron concentration increases. The coefficient in Eq. (16) is determined so that the diffusivity matches the above value. The molar density of the gas can be calculated from the ideal gas law:

$$c = \frac{P}{RT} \quad (17)$$

Few sources are available about the oxidation rate of pure iron. A rough estimate can be inferred from the experimental results of Robertson and Jenkins (1970). The reaction controlled experiment was conducted by levitating a 1 g sphere iron in an ample supply of oxygen. The rate corresponds to an oxidation flux of iron of $0.36 \text{ g}_{\text{Fe}} \text{ cm}^{-2} \text{ s}^{-1}$ at temperature of 1600°C . The oxygen flux is thus about $3.2 \times 10^{-3} \text{ mol cm}^{-2} \text{ s}^{-1}$.

The absorption distribution of the laser power for different cutting front geometries has been studied by Petring, *et al.* (1988). For TEM₀₀ mode and circular polarized laser beam, the absorption coefficient is about 30% for inclination between 80 and 88 degrees, but reduce to about 10% when inclination increases to 90 degree. Here a constant of 30% is used for calculation. The reaction heat is taken as $\Delta H_r = -257.58 \text{ kJ/mol}$ (of iron).

2.4 Numerical Scheme

A control-volume based discretization method is utilized to solve the coupled convection-diffusion problem. The detailed description of discretization of the parabolic governing equation is given by Patankar (1980). The power-law scheme is used, which provides a good representation of the convection-diffusion behavior. The source term also includes the values of the previous time step if the calculation is time dependent. The temperature or concentration dependent coefficients are linearized between each time step to facilitate the convergence. The discretization equation groups are solved by a line-by-line tridiagonal matrix algorithm.

3. Calculation Results and Analyses

3.1 Steady State Results

Figure 2 shows the temperature profile along the calculation domain with different oxygen purity and different cutting speed respectively. Since the heat source is at the gas-solid interface, the temperature is highest at the interface. The temperature quickly drops when it is close to the center of the gas stream because of highly convective effect. Inside the material the temperature profile has less gradient and the heat affected zone (HAZ) can be estimated accordingly. If the HAZ is taken above 800 °C, which corresponds to a transitional temperature of microstructure of mild steel, the HAZ is about 0.7 mm for parameters used in calculation.

Figure 3 depicts the profile of oxygen concentration with different oxygen purity. A small decrease of purity brings about a large drop of oxygen concentration at the interface, thus greatly reducing the produced reaction energy. Figure 4 shows the effects of oxygen purity on cutting speed. The cutting speed is highly sensitive of small levels of

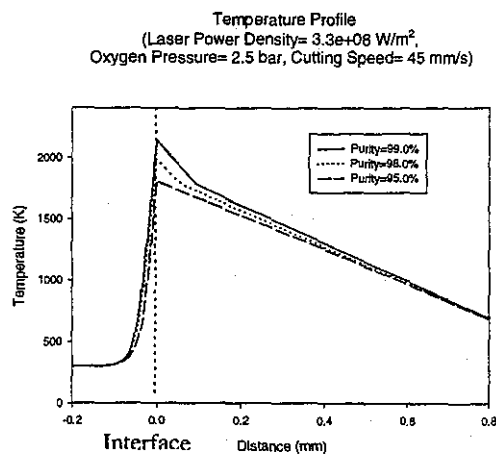


Figure 2: The calculated temperature profile with different oxygen purities

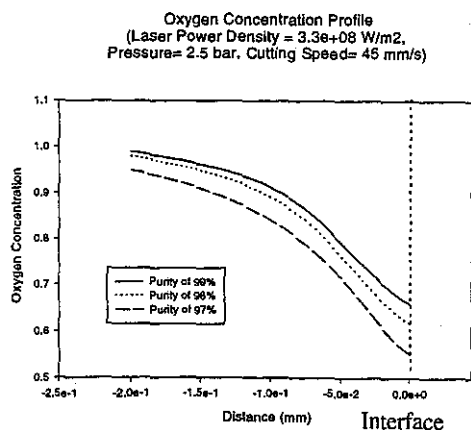


Figure 3: The calculated oxygen concentration profile with different oxygen purity

contamination in the oxygen jet, which is consistent with the experimental results given by Powell, *et al.* (1992). This result came from the quickly accumulated gas diffusion film when oxygen impurity increases. The effects of various gaseous impurities are also shown in Figure 4. The impurity of He has less effect than that of N₂ because its smaller molecular weight and diffusion volume result in a larger diffusion coefficient, and consequently more oxygen flux for reaction, which is confirmed by the experiment observation (Gabzdyl and Morgan, 1992).

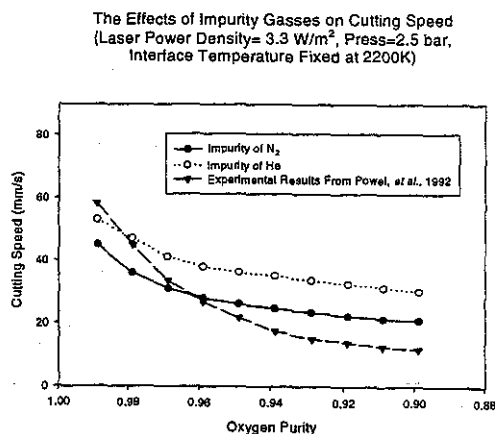


Figure 4: The effects of oxygen purity on cutting speed

3.2 Striation Formation

Oxygen-assisted laser cutting of mild steel will result in a regularly-spaced pattern on the cut surface. A commonly accepted explanation is that the striations are related with the cyclic oxidation which has been observed to undergo ignition, burning and extinction cycle (Arata, 1979; Ivarson, *et al.*, 1994). Another explanation is based on hydrodynamic instability (Vicanek, *et al.*, 1986). It is further pointed out that striation formation is associated with the oxide layer which is hydrodynamic unstable (Chen and Yao, 1997). Since the diffusivity of the oxides is much larger than that of the gas (about 10^4 times), the formation of oxide layer will greatly hinder the oxidation process. But the oxide layer is unstable and will rupture or generate waves under hydrodynamic forces of the gas jet. The cyclic growth-removal of the oxide layer will cause the fluctuation of temperature and molten layer, which brings about striation patterns. Since the behavior of the oxide layer under the effect of melt ejection is not well understood, a reasonable assumption is that the growth of the oxide layer for the diffusion controlled process follows the well known parabolic law (Chen and Yao, 1997).

This simulation assumes that the oxide layer grows following the parabolic law, then is removed because of the hydrodynamic instability. After it is removed, the oxide layer starts to grow again. The period of this growth-removal cycle is given from the calculation of the instability theory (Chen and Yao, 1997), which correlates reasonably with experimental results. Figure 5 shows typical calculated front temperature fluctuation. Since the coefficient of the parabolic growth is not readily available, it is calibrated so that the temperature fluctuation is around a level known from experiments. When the oxide layer starts to grow, the oxidation slows down because of the high resistance of the oxide layer to the oxygen diffusion, and the temperature starts to drop. Once the oxide layer is removed, the temperature quickly picks up due to a sudden increase of oxygen flux and reaction energy. This type of temperature fluctuation during a cut process has been recorded via the light intensity change picked up by high speed photograph (Di Pietro, Yao and Chen, 1997).

When the cutting speed varies, the front temperature and the striation period vary accordingly. Figure 6 shows the temperature fluctuation range decreases with cutting speed. When the cutting speed increases, the temperature fluctuation range decreases. It is reasonable to expect that the decrease of the temperature fluctuation range relates to the decrease of the striation depth. This is confirmed by the experimental measurement of depths shown on the same figure. The experiments are

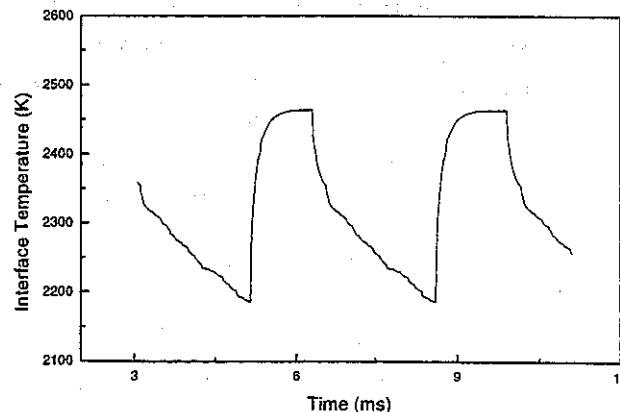


Figure 5. The transient interface temperature fluctuation

carried out by the same authors and its detail conditions are seen in Chen and Yao's paper (1997). The gas pressure also has great influence on the front temperature and striation period. When gas pressure increases, so does the molar density of the oxygen, which increase the oxygen flux and enhance the reaction. The striation period is also affected through the change of shear force and gas velocity. Figure 7 shows the temperature fluctuation range against pressure. The increase of pressure brings about the increase of temperature fluctuation range, which corresponds to increase of striation depth measurements, as shown in the same figure.

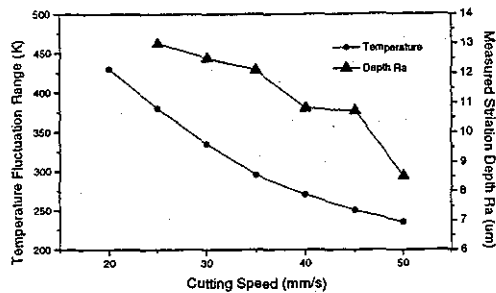


Figure 6: Temperature fluctuation range and measured striation depth vs. cutting speed

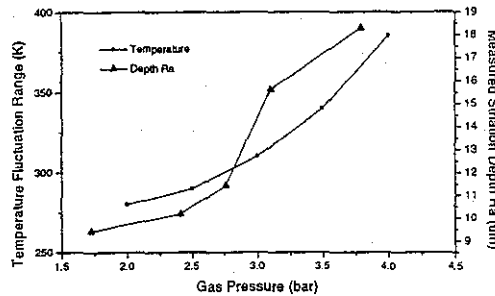


Figure 7: Temperature fluctuation range and measured striation depth vs. gas pressure

4. Concluding Remarks

The above calculation results and analyses show that the model developed in this paper can theoretically describe the process of the oxygen-assisted cutting of mild steel. The numerical simulation can quantitatively predict the effects of the oxidation process. The numerical results confirms that a small amount of oxygen impurity will greatly reduce the oxygen diffusion to the melt phase and reduce the oxidation energy. This agrees with the experimental investigation that the cutting speed is greatly reduced when the oxygen impurity increases by a small amount. The striations are related with the unstable behavior of the oxide layer since the oxidation energy is very sensitive of the oxide layer which has large resistance to the diffusivity. With the oxide layer oscillation based on the instability theory, the striation phenomenon can be simulated by transient temperature fluctuation. The trends of the temperature fluctuation range versus cutting speed and the gas pressure are consistent with the experimental results.

References

- Arata, Y., *et al* (1979), *Trans. JWRI*, Vol. 8(2), 1979, pp. 15-26.
- Chen, K., and Yao, Y.L. (1997), *MED-Vol. 6-1, Manufacturing Science and Technology, ASME 1997*, Vol. 1, pp. 301-307.
- Di Pietro, P., Yao, Y. L., and Chen. K. (1997), *Technical Papers of NAMRI*, 1997, pp. 105-110.
- Di Pietro, P., Yao, Y. L. (1995), *Int. J. Mach. Tools Manufact.*, 35(5), pp. 673-688.
- Gabzdyl, J. T. and Morgan, D. A. (1992), *ICALEO'92*, pp. 443-448.

- Ivarson, A., *et al.* (1994), *J. of Materials Processing Technology*, Vol. 40, pp. 359-374.
- Nickolas, J. T. (1995), *Transport and Chemical Rate Phenomena*, Gordon and Breach Publishers.
- Patankar, S. V. (1980), *Numerical Heat Transfer and Fluid Flow*, Taylor & Francis Publishers.
- Powell, J., *et al.* (1992), *ICALEO'92*, pp. 433-442.
- Petring, D. *et al.* (1988), *SPIE*, Vol. 1020, High Power CO2 Laser Systems and Applications, 1988, pp. 123-131.
- Robertson, D. G. C., and Jenkins, A. E. (1970), *Heterogeneous Kinetics at Elevated Temperatures*, G. R. Belton and W. L. Worrel ed., Plenum Press, New York.
- Schlichting, H. (1979), *Boundary-Layer Theory*, McGraw-Hill Book Company, New York.
- Schuoocker, D., and Abel, W. (1984), *Proc. of SPIE, Industrial Applications of High Power Lasers*, Vol. 455, pp. 88-95.
- Schuoocker, D. (1986), *Appl. Phys. B*, 40, pp.9-14.
- Vicanek, M., *et al.* (1986), *J. Phys. D: Appl. Phys.*, Vol. 20, pp. 140-145.

Meet the Authors

Kai Chen is a Ph.D. student in the Department of Mechanical Engineering at Columbia University. He received M.S. degree from Dartmouth College in 1996. Y. Lawrence Yao is an Associate Professor in the Department of Mechanical Engineering at Columbia University. He received his M.S. and Ph.D. from University of Wisconsin-Madison in 1984 and 1988, respectively.

PROCEEDINGS
of the
**LASER MATERIALS PROCESSING
CONFERENCE**

ICALEO'97

**LIA Volume 83
Part 1**

CO-CHAIRS:

Rémy Fabbro, Laboratoire LALP, Arcueil, France

Aravinda Kar, University of Central Florida, Orlando, FL

Akira Matsunawa, Osaka University, Osaka, Japan

Published by the LIA

Laser Institute of America
12414 Research Parkway, Suite 125
Orlando, FL 32826